Science Advances
AAAS

advances.sciencemag.org/cgi/content/full/4/12/eaau9245/DC1

# Supplementary Materials for

## Fluorinated solid electrolyte interphase enables highly reversible solid-state Li metal battery

Xiulin Fan, Xiao Ji, Fudong Han, Jie Yue, Ji Chen, Long Chen, Tao Deng, Jianjun Jiang, Chunsheng Wang*

*Corresponding author. Email: cswang@umd.edu

Published 21 December 2018, *Sci. Adv.* **4**, eaau9245 (2018)
DOI: 10.1126/sciadv.aau9245

**This PDF file includes:**

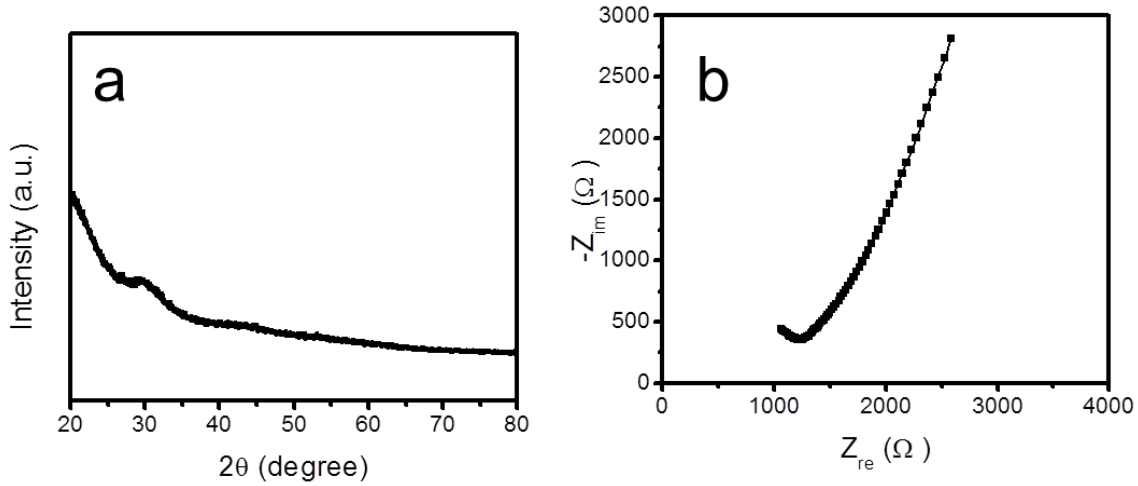


**Fig. S1. XRD pattern and the electrochemical impedance spectra of the as-synthesized LPS SSE.** XRD pattern (**a**) and the electrochemical impedance spectra (**b**) of the as-synthesized LPS solid state electrolyte. The as-synthesized LPS solid state electrolyte showed an amorphous structure with an ionic conductivity of $2.6 \times 10^{-4}$ S/cm at room temperature. The bump at about 30° in the XRD pattern is from the protected tape during XRD characterization. The impedance spectra were obtained with Pt|LPS|Pt cell.

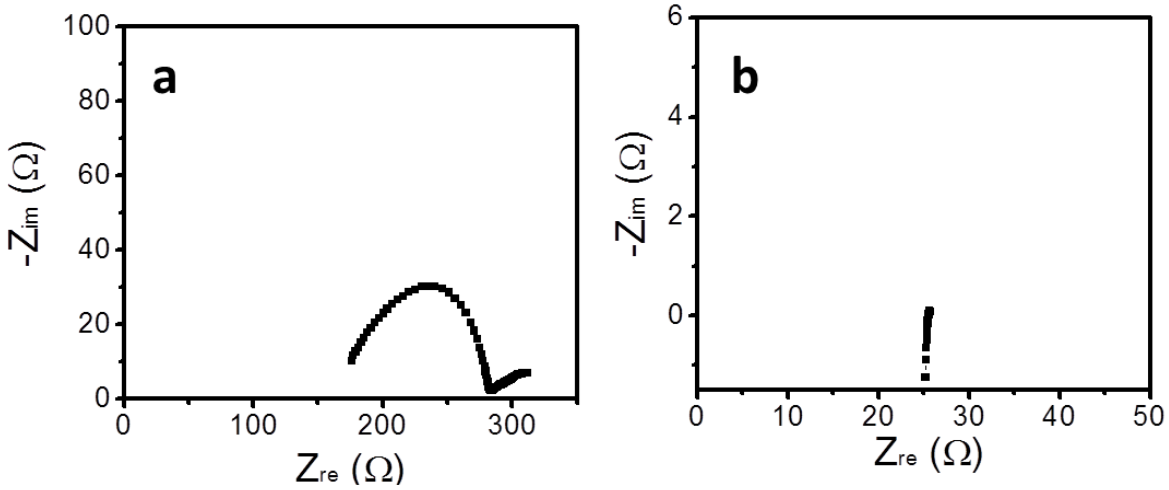


**Fig. S2. Impedance plot of the Li|LPS|Li cell before cycling and after cycling.** Impedance plot of the Li|LPS|Li cell before cycling (**a**) and after cycling for 90 hours (**b**) at 0.3 mA $cm^{-2}$ at 25 °C.

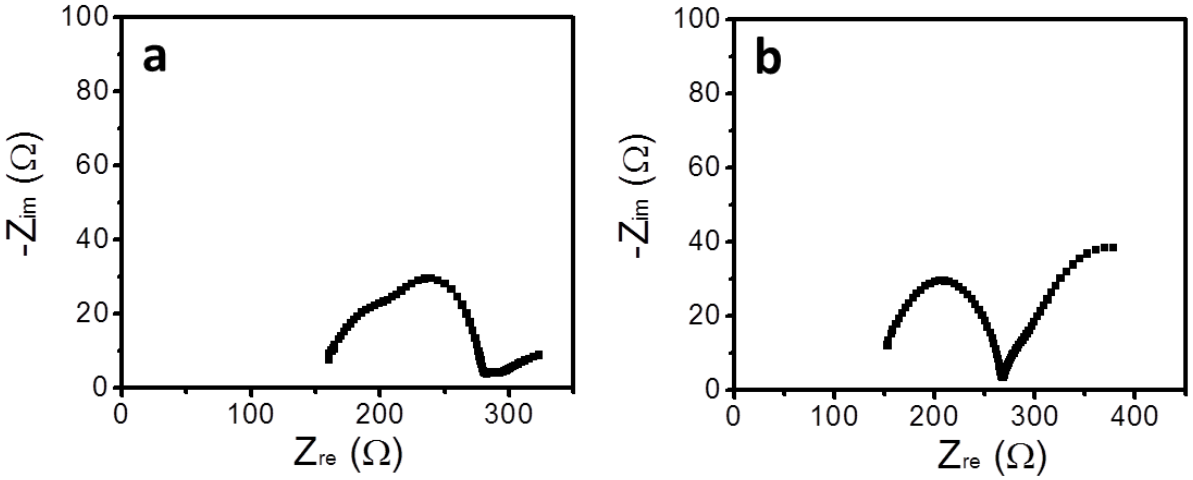


**Fig. S3. Impedance plot of the pretreated Li|LPS|Li cell before cycling and after cycling.** Impedance plot of the pre-treated Li|LPS|Li cell before cycling (**a**) and after cycling for 300 hours at 0.3 mA/cm$^2$ at 25 °C (**b**).

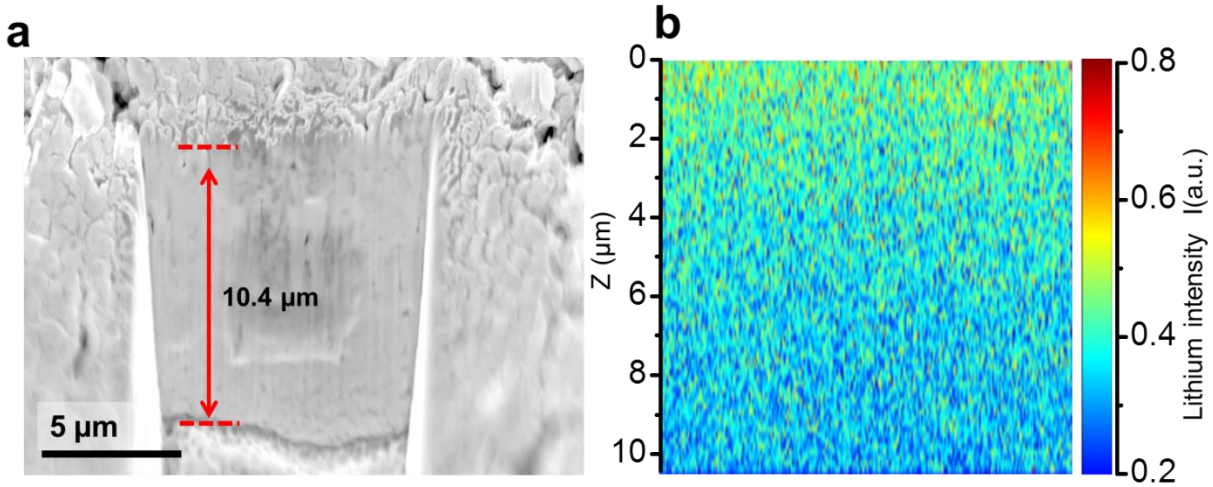


**Fig. S4. ToF-SIMS analysis of the positive ions for the interface of the LPS.** (**a**) SEM image of the cycled LPS SSE after $Ga^+$ beam sputtering; (**b**) the Li element distribution with depth.

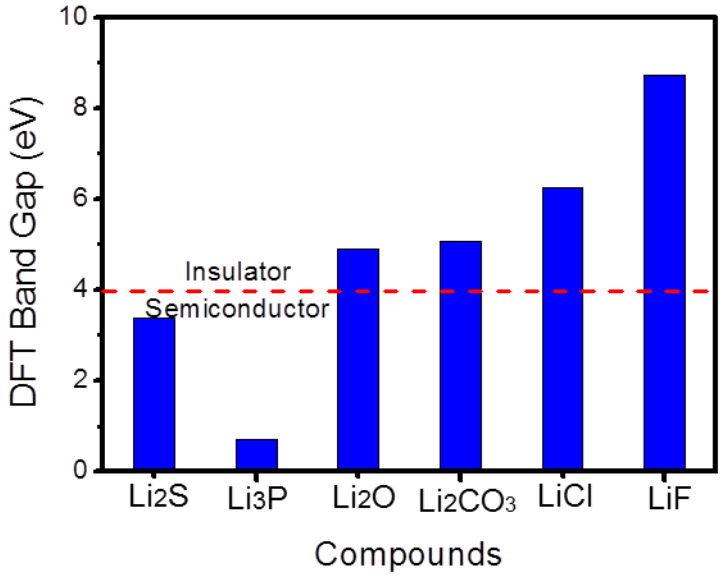


**Fig. S5. Comparison of the bandgaps for different materials.** Generally, 4.0 eV is regarded as the dividing line between the semi-conductors and the insulators *(46)*. The band gap of the Si and Ge is 1.1 eV and 0.66 eV, respectively. Obviously, the in situ formed $Li_3P$ during Li plating/stripping cannot effectively block the electron transport in the as-formed passivation layers between the solid state electrolyte and the Li metal because of the low band gap of 0.7 eV. The values are obtained from Materials Projects (*47*).

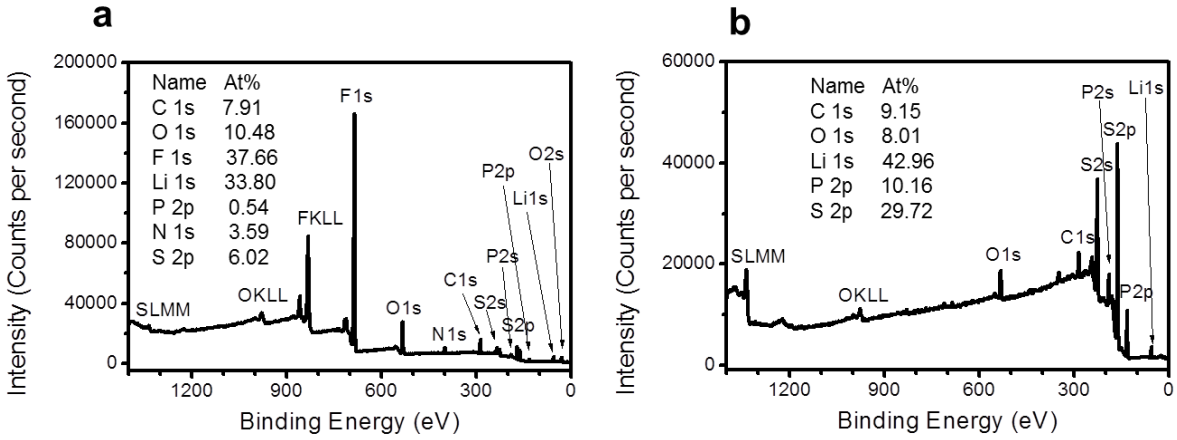


**Fig. S6. XPS spectra of cycled LPS recovered from the pretreated SSE cell and untreated cell.** XPS spectra of cycled LPS recovered from the pre-treated SSE cell (**a**) and un-treated cell (**b**). Compared with the untreated cell, significantly high F-rich species can be detected for the LPS recovered from the pre-treated SSE cells.

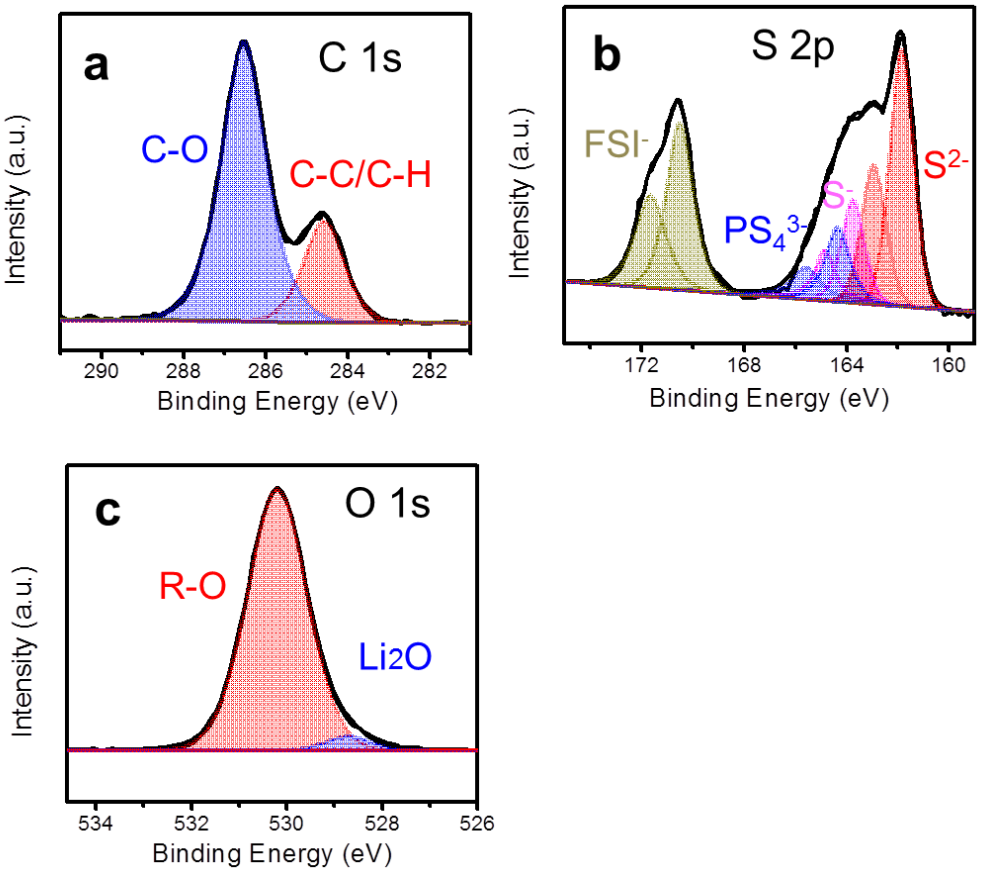


**Fig. S7. SEI components in the LPS recovered from the pretreated cell by XPS.** (**a**) C 1s spectra; (**b**) S 2p spectra; (**c**) O 1s spectra.

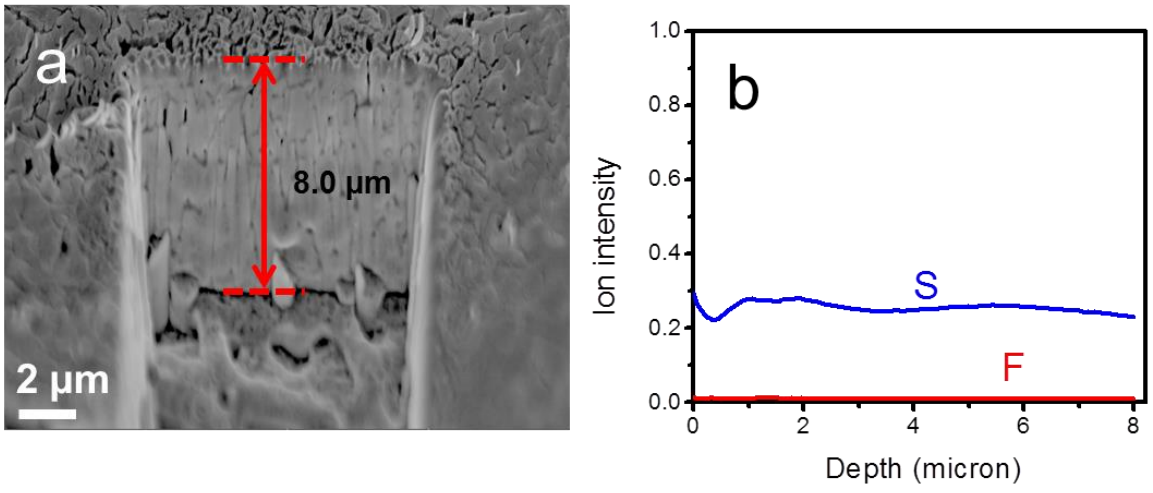


**Fig. S8. ToF-SIMS analysis of the negative ions for the interface of the cycled LPS SSE.** (**a**) SEM image of the cycled LPS SSE after $Ga^+$ beam sputtering; (**b**) the anion element distribution (S and F) with depth.

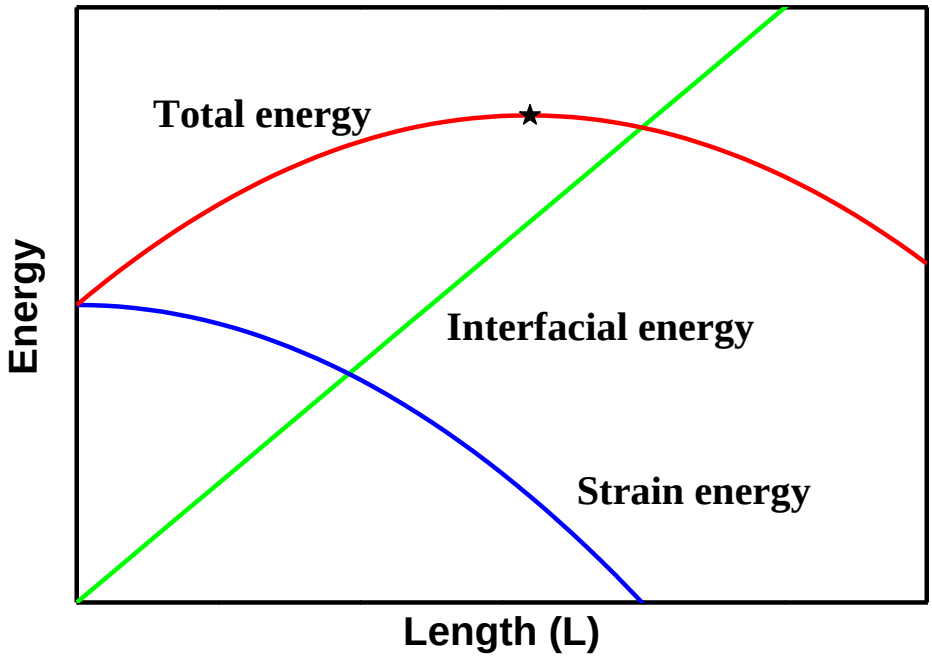


**Fig. S9. Relationship between the total energy, the interfacial energy, and the strain energy with the dendrite length during the dendrite formation in the SSEs.** The black star indicates the failure length.

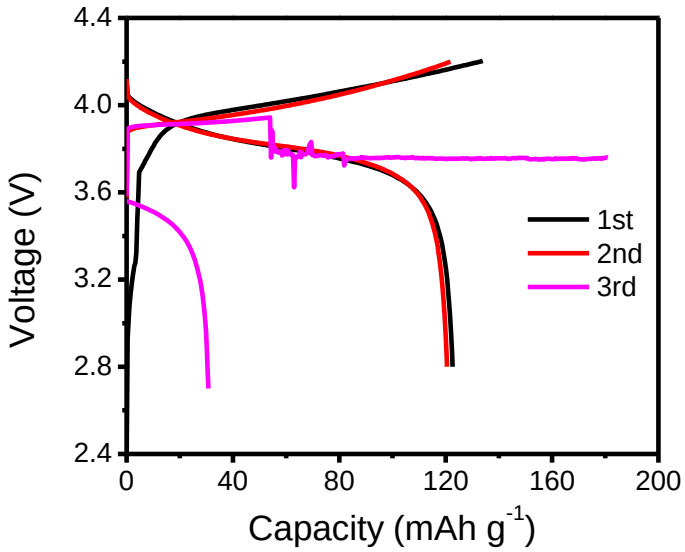


**Fig. S10. Charge/discharge curves for the Li|LPS|LCO cell.** The current density is 0.3 mA $cm^{-2}$. At the 3$^{rd}$ cycle, short-circuit occurs with the sudden drop of the charging potential. As the charging capacity reached 180 mAh $g^{-1}$, we forced the cell to discharge. Only about 30 mAh $g^{-1}$ was delivered.

**Note S1. Critical Li dendrite length and the Li dendrite suppression ability for the SSEs.**

To evaluate the effect of SEI layer on suppression the Li dendrite, the criterion for Li dendrite growth in SEI is defined based on the energy analysis. When Li dendrite grows along the grains of brittle SEI, the work is needed to form new interface while the strain energy at the tip of the grain boundary will be released. According to the Griffith's energy-based analysis,(*48*) the total energy ($E_{total}$) needed for Li dendrite growth can be expressed as the summation of interface energy ($E_{interface}$) and strain energy ($E_{strain}$) as shown in following Eq. 1

$$E_{total} = E_{interface} + E_{strain} \quad (1)$$

the interfacial energy is expressed as

$$E_{interface} = 2\gamma LB \quad (2)$$

While γ represents the interfacial energy required to form new Li/SEI interface per unit surface area. The surface area is L*B where L is the interface length and B is the part thickness. And the released strain energy can be calculated as

$$E_{strain} = \frac{\sigma^2}{2E}V - \frac{\sigma^2}{2E}B\pi L^2 \quad (3)$$

where σ is the stress at the tip of crack or grain boundary, E is the bulk modulus and V represent the volume.

Hence, the total energy can be expressed as (as shown in Figure S7)

$$E_{total} = 2\gamma LB + \frac{\sigma^2}{2E}V - \frac{\sigma^2}{2E}B\pi L^2 \quad (4)$$

Relationship between the total energy, interfacial energy and the strain energy with the dendrite length during the dendrite growth in the SSEs is shown in Figure S9.

In order to find the critical length where the unstable Li dendrite will spontaneously grow, the total energy with respect to the length is differentiated and then the derivative is set to be zero

$$\frac{dE_{total}}{dL} = 2\gamma B - \frac{\sigma^2}{E}B\pi L = 0 \quad (5)$$

Hence, the critical length of Li dendrite $L_c$ can be expressed as

$$L_c = \frac{2\gamma E}{\pi\sigma^2} \quad (6)$$

$L_c$ is the minimum Li dendrite length before Li dendrite is stable and begins to grow. For a given strain (σ), the critical length of Li dendrite increases with the γE of the SEI component. In this work, the calculated value of γE is used to evaluate the effect of SEI layer on suppression of the Li dendrite in SSEs.

**Note S2. Computational model and method for the interfacial energy.**

To calculate the interfacial energies, the same method reported by Holzwarth is used, the typical model are shown in Figure 5 e and f.(*34*) Generally, the interface energy ($\gamma_{ab}$) between two materials a and b is defined as the energy difference between an interface system and the bulk energy of the two materials that comprise it for a given $\Omega$

$$\gamma_{ab}(\Omega) = \frac{E_{ab}(\Omega, A, n_a, n_b) - n_a E_a - n_b E_b}{A} \tag{7}$$

where $E_{ab}$ is the total energy of the interface system, and it depends on the formula units of materials a and b comprise the interface ($n_a$ and $n_b$ respectively), as well as the configuration ($\Omega$) and interfacial area $A$. $E_a$ and $E_b$ denote the energy per formula unit for bulk a and b respectively. However, it is expensive to evaluate the energy of realistic trial configuration $\Omega$. For the consideration of efficiency, we used the periodic ordered phase ($\Omega$) to approximate $\Omega$.
For a semi-coherent interface, there is some degree of lattice mismatch between the two phases. The imposing periodic boundary conditions to the simulation system will result in lattice strain to bring the two lattices into alignment. Consequently, according to Eq.(7), the interface energy calculated in the periodic cell depends on $n_a$ and $n_b$

$$\gamma_{ab}(\Omega, n_a, n_b) = \frac{E(\Omega, A, n_a, n_b) - n_a E_a - n_b E_b}{A} \tag{8}$$

The terms of Eq.(8) are defined identically to those Eq.(7). The tilde is used to label the periodic cell. Because of the lattice strain, $\gamma_{ab}$ does not converge with respect to system size in the direction perpendicular to the interface. Subtracting the strain energy from $\gamma_{ab}$ is equivalent to computing the interface energy in the coherent limit as following definition

$$\gamma_{ab}^{\lim}(\Omega) = \frac{E_{ab}(\Omega, A, n_a, n_b) - n_a E_a - n_b E_b - E_{str}(\Omega, n_a, n_b)}{A} \tag{9}$$

herein, $E_{str}$ denotes the strain energy induced by the lattice mismatch, $\Omega$ is the interface configuration in the periodic cell. By subtracting the strain energy, the $\gamma_{ab}^{\lim}(\Omega)$ does not depend on $n_a$ and $n_b$, and thus converges much better with respect to system size and provide a better estimate of $\gamma_{ab}(\Omega)$.

In our manuscript, we calculated $\gamma_{ab}$ for several interface systems which had the same $\Omega$ and had their lattices fixed to the bulk values of SSEs or SEI components, but which had different amounts of Li metal. For these Li SSEs or SEI interface systems beyond the value of $n_{Li}$, the relation can be obtained using Eq.(10)

$$\gamma_{ab}(\Omega, n_b) = \gamma_{ab}^{\lim}(\Omega) + n_b \sigma \tag{10}$$

where $\sigma$ is a constant related to the strain energy in Li metal. According to Eq. (10), the models (figure 5e and f) are constructed and Figure 5c is plotted.